Multiple-Antenna Channels from a Combined Physical and Networking Perspective

Ada S. Y. Poon, David N. C. Tse and Robert W. Brodersen
University of California, Berkeley
{sypoon, dtse, rb}@eecs.berkeley.edu

***Abstract*— The benefits of multiple-antenna systems in a wireless network are threefold — increase data rate, improve reliability against channel fading, and perform interference management. All these benefits can be realized simultaneously; however, there is a limit. This limit depends on physical parameters, including the size of the wireless device, scattering characteristics of the channel and the operating frequency. In this paper, we will propose an indoor channel model that captures this set of physical parameters and the physical distribution of nearby users. Based on this model, we will show how the impact of the physical environment can be abstracted in a high level study of the performance tradeoff of multiple-antenna systems in a wireless network.**

I. Introduction

In a wireless channel, transmitted data is first radiated from the transmitting antenna into free space and carried by propagation waves. The course of the waves will then be affected by the objects in the channel. Eventually, a fraction of the waves that orients towards the receiver, is intercepted by the receiving antenna. The description is simple but it does bring out two important quantities capturing the promise of a multiple-antenna channel. First, the amount of possible propagation paths from the transmitter to the receiver created by the channel objects. Second, how many of these paths can be resolved by the transmitting and receiving antenna arrays. We term the former quantity as the *extent of channel scattering*, Ω and the latter as the *resolvability of antenna array*, L. In this paper, we will first quantify them and then derive the multiplexing limit of a multiple-antenna channel in terms of these two quantities. Our result is analogous to the WT degrees of freedom in the classic Shannon's AWGN channel. Thus, for a multiple-antenna channel with transmission bandwidth of W, transmission time of T, antenna resolvability of L and channel scattering intensity of Ω, there is asymptotically $WTL\Omega$ degrees of freedom.

The expression reflects a separation of the impact of antenna and channel characteristics on the performance limits. This separation is especially crucial for designing a multiple-antenna system. As now the controllable quantities, like the number of antennae and their configurations, are separated from the uncontrollable quantity, the channel itself. This would allow system designer to better understand and optimize the system performance.

All these are built upon a proposed change of coordinates to the *beam-angle* coordinate system which is used in antenna theory to study the directional properties of radiating systems. We have adapted it to model the multiple-antenna channel. In this coordinate system, we can separate the influence of the channel and the transmit-receive antenna system. In addition, since the proposed coordinate system captures the directional properties of both transmitting and receiving signals, the physical distribution of other users in the channel will become more apparent. Hence, this proposed coordinate system facilitates the study of the performance limits of multiple-antenna channels in a networked environment.

In the next section, we will present the proposed channel model, and contrast it with the popular channel models in the literature. Based on this model, we will derive the multiplexing limits for various propagation scenarios in Section III. From which, we will elucidate the impact of channel and transmit-receive antenna systems on the performance limits of a multiple-antenna channel. To justify the multiplexing limits derived, in Section IV, we will apply the proposed model to evaluate different antenna array configurations and determine the optimum number of antenna elements for a given size of wireless device in a given channel. In Section V, we will apply the multiplexing limit results to investigate the benefit of using higher operating frequencies. The computation involved is straightforward but it does give good intuition on which frequency band is more optimum for a given channel. To end this paper, we will show how the proposed approach extends to a network of multiple-antenna systems in Section VI. Finally, a summary of this paper is included in Section VII

II. Channel Model

As mentioned, the promise of a multiple-antenna channel hinges on signal radiation from the antenna system and wave propagation in the channel. To understand the full scope of this relationship, a channel model that abstracts these underlying electrodynamic mechanisms is desired. Existing models are inadequate in this aspect. Currently, there are two widely used approaches. Both of which assume a given number of transmit and receive antennae. The first model focuses on modeling the channel gains by the statistics and the correlation among transmit-receive antenna pairs. This model is analytically tractable, and hence, is used intensively in capacity analysis [1] and in the design of space-time codes [2], [3]. However, it fails to capture the scattering characteristics of the channel and the physical distribution of nearby users. The second model, on the other hand, has a more accurate descriptions of the propagation environment as it models the channel gain on each propagation path which is characterized by its angle of departure and angle of arrival. However, it fails to capture the clustering phenomenon of the paths and the resolvability of the transmit-receive antenna system.

To cope up with these inadequacies, we propose a channel model that accounts for the underlying mechanisms for radiation and propagation separately. Their ultimate connection is through the use of a common coordinate system – beam-angle coordinates.

A. Radiation Abstraction

Basically, any time-varying current will radiate electromagnetic waves. The role of an antenna system is to accomplish the job in a controlled and efficient manner. By varying the signals on the antenna system, the strength of the radiated electromagnetic waves propagating in various directions will be changed accordingly. Dating back to 1949, Booker and Clemmow [4] pointed out that the field at all points in front of a one-dimensional antenna system (*aperture*) of any excitation distribution (*aperture distribution*) can be regarded as arising from an aggregate of plane waves traveling in various directions. The amplitude and phase of the waves, as a function of their direction of propagation, constitutes an *angular spectrum*. When it is appropriately expressed, it is the *Fourier transform* of the aperture distribution without any approximation. The field at a point distant away is simply the linear combination of these plane waves. If the distance is sufficiently large, then only the plane waves with direction of propagation pointing towards that observation point survive. This concept of angular spectrum and aperture distribution is widely applied in the area of antenna synthesis. In this paper, we are applying it to model the radiation mechanism in a multiple-antenna channel.

An aperture, in our definition, is any radiating surface on which one can put as many antenna elements as desired. This is in contrast to the conventional multiple-antenna channel model where the number of antenna elements is given. The aperture distribution abstracts the transmitted information across the aperture and is normalized to the wavelength. Consider a linear aperture oriented along the z-axis and wave propagating on the y-z plane (that is, $\phi = 90°$.) Suppose $x(z)$ is the aperture distribution. Then, from Maxwell's equations, the electric field at a distance r and an elevation direction of θ away from the source, is approximated by

$$\mathcal{E}(r,\theta) \approx \frac{j\eta}{2}\frac{e^{-j2\pi r/\lambda}}{r}\int_{-L/2}^{L/2} x(z)\, e^{j2\pi\cos\theta z}\, dz \qquad (1)$$

where L is the length of the aperture normalized to wavelength. The approximation is due to the far-field assumption. The first two factors in the expression depend on the electromagnetic properties of the channel, path loss and phase delay. The third factor which gives the angular spectrum, abstracts the transmitted data radiated in the θ-direction. Define $\alpha = \cos\theta$ and denote the angular spectrum by $s(\alpha)$. Then, we have the following relationship,

$$s(\alpha) = \int_{L/2}^{L/2} x(z) e^{j2\pi\alpha z}\, dz \qquad (2)$$

From the expression, we see that the aperture distribution and angular spectrum have a Fourier transform relationship constrained to the interval $[-L/2\ \ L/2]$. Suppose F is the Fourier operator and P_S denotes the orthogonal projection in the Hilbert space $\mathcal{L}_2(-\infty,\infty)$ onto the subspace S. Then the radiation mechanism can be abstractly modeled by the operator

$$Q_L = F^\dagger P_L F \qquad (3)$$

where † denotes the Hermitian operation. Furthermore, we call the α-coordinate the beam-angle coordinate.

B. Propagation Abstraction

To abstract the propagation mechanism, two observations from recent indoor wireless channel measurements are noteworthy. First, received signals are not only clustered along the time axis [5], but also in the directions of departure and arrival as well [6], [7], [8]. It occurs in a wide range of frequencies and bandwidth. Second, the path loss exponent varies only from 2 up to 6 [9]. Typical value is between 2 and 4. This implies that signals are mostly bouncing once and up to twice by the channel objects before reaching the receiver.

The clustering phenomenon is the result of scattering from channel objects of various dimension, roughness and electromagnetic properties along the propagation path connecting the transmitter and the receiver. Broadly speaking, there are two major cases to differentiate. First, when the scattering object is large and smooth, the response is specular in nature. Example is the back-wall reflection. In brevity, the angles of incidence and reflection are equal and coplanar. Let α and β be the reflected and incident directions. Note that α and β are the cosine of the elevation angles. Then the response is given by

$$\delta(\alpha-\alpha_0)\,\chi_{\Omega_R}(\alpha)\chi_{\Omega_T}(\beta) \qquad (4)$$

where $\chi_S(\cdot)$ is the characteristic function for the subspace S. α_0 depends on β and conforms to the Snell's law of reflection. Ω_R and Ω_T are the solid angle subtended by the scattering object from the transmitting point and the observation point respectively. All these parameters depend on the scattering object's geometry, electromagnetic properties and its distance from the transmitting and observation points.

The second case is when the scattering object is small relative to the wavelength, it acts like a secondary source and functions like a *passive relay*. It absorbs energy from the incident wave and re-radiates it to all the directions. Thus, the response is diffused and stochastic in nature. Examples are scattering from furniture, diffraction from door-way openings and transmission through soft partitions. Due to its role as a second radiator, we model the diffuse response as a random processes with zero mean,

$$h(\alpha,\beta)\chi_{\Omega_R}(\alpha)\chi_{\Omega_T}(\beta) \qquad (5)$$

where $h(\alpha,\beta)$ is a zero-mean, two-dimensional random processes. Similarly, Ω_R and Ω_T are the solid angle subtended by the scattering object from the transmitting point and the observation point respectively.

As a result, the response of any channel object is modeled as a superposition of specular and diffuse responses. For example, scattering from a large but rough surface, will have a specular component as if the surface is flat and smooth, and a diffuse component depending on the roughness and orientation of the surface.

To fully model the propagation mechanism, we have to consider the bouncing frequency of the propagation path connecting the transmitter and the receiver. If all the propagation paths bounce only once, then the overall response will be

$$\sum_{m=1}^{M} h_m(\alpha,\beta)\,\chi_{\Omega_{Rm}}(\alpha)\chi_{\Omega_{Tm}}(\beta) \tag{6}$$

The transmitting directions will have a strong coupling with the receiving directions. However, channel measurements reveal the possibility of bouncing twice or more. In this case, each scattering point in the second scattering object can be treated as an observation point for the first scattering object. Likewise, it absorbs energy scattered from the first scattering object and then re-radiates it. Consequently, the overall channel response shows a weaker coupling between the transmitting and receiving directions. Mathematically, the overall response can be expressed as

$$\sum_{n=1}^{M_R}\sum_{m=1}^{M_T} h_{nm}(\alpha,\beta)\,\chi_{\Omega_{Rn}}(\alpha)\chi_{\Omega_{Tm}}(\beta) \tag{7}$$

$\{\Omega_{Tm}\}$ is the set of solid angle subtended by the scattering objects being illuminated by the transmitting antenna system and M_T is its cardinality. Similarly, $\{\Omega_{Rn}\}$ is the set of solid angle subtended by the scattering objects as observed from the receiving antenna system and M_R is its cardinality. $h_{nm}(\alpha,\beta)$ is the corresponding response in between. It is guided by the two scattering mechanisms discussed and the number of bounces involved. For example, in the line-of-sight channel, the response would be

$$\delta(\alpha-\beta)\chi_{\Delta}(\beta) \tag{8}$$

where Δ is the angle subtended between the transmit-receive antenna system.

In terms of the operators defined, the overall response can be modeled as

$$\sum_{n=1}^{M_R}\sum_{m=1}^{M_T} P_{\Omega_{Rn}} H_{nm} P_{\Omega_{Tm}} \tag{9}$$

where the kernel of H_{nm} is $h_{nm}(\alpha,\beta)$ for all n and m.

C. Complete Model

By the Lorentz reciprocity theorem for antennae, the reception mechanism can be modeled like the radiation mechanism. Thus, the complete angular response in the far-field region will be

$$Q_{L_R}\sum_{n=1}^{M_R}\sum_{m=1}^{M_T} P_{\Omega_{Rn}} H_{nm} P_{\Omega_{Tm}}\, Q_{L_T} \tag{10}$$

where L_T and L_R are the length of the transmitting and receiving apertures normalized to wavelength respectively. $Q_{L_R}P_{\Omega_{Rn}}$'s and $P_{\Omega_{Tm}}Q_{L_T}$'s have only a finite number of significant eigen-modes. Moreover, M_T and M_R are finite, therefore, for a given size of the wireless device if one can put any number of antenna elements on it, and for a given propagation scenario, there is only a finite number of useful modes for information transmission. In the next section, we will work out this limit. It is important to note that our proposed channel model assumes a given length of antenna system as opposed to a given number of antenna elements on the antenna system. Furthermore, it does not use the correlation among antenna elements to reflect the channel condition. Instead, the set of non-zero angular spectra, Ω_{Rn}'s and Ω_{Tn}'s and the coupling between them designate the channel condition. This would allow us to study the effect of antenna system and propagation channel on the performance limits separately.

III. Multiplexing Limits

In this section, we will consider three different propagation scenarios — line-of-sight, specular single-bounce and diffuse multi-bounce. In all the scenarios, we assert that the sets of non-zero solid angles are known. As we believe that these intervals are changing much slower than the channel fading effect. The main results are summarized in Theorem 1.

A. Main Results

Theorem 1: Let SNR denote the transmit signal-to-noise ratio. Define $\Omega_T = \bigcup_n \Omega_{Tn}$ and $\Omega_R = \bigcup_n \Omega_{Rn}$.

(a) Line-of-sight Channel. The channel response is given by

$$Q_{L_R} P_{\Delta} Q_{L_T}$$

and the capacity C_{LOS} is

$$C_{LOS} = \log_2\left(1 + L_T L_R |\Delta|^2 \mathsf{SNR}\right) \tag{11}$$

(b) Specular Single-bounce Channel. The channel response is given by

$$Q_{L_R} P_{\Omega} Q_{L_T}$$

Assume $L_T = L_R = L$, $M_T = M_R$ and $\Omega_R = \Omega_T = \Omega$. Define $\mathsf{SNR}_b = \mathsf{SNR}/(L|\Omega|)$. Then the channel capacity C_{SP} satisfies

$$\lim_{L|\Omega|\to\infty} \frac{C_{SP}}{L|\Omega|} = \log_2(1+\mathsf{SNR}_b) \tag{12}$$

(c) Diffuse Multi-bounce Channel. The channel response is given by

$$\sum_{n=1}^{M}\sum_{m=1}^{M} Q_{L_R} P_{\Omega_{Rn}} H_{nm} P_{\Omega_{Tm}} Q_{L_T}$$

Assume $L_T|\Omega_T| = L_R|\Omega_R|$ and $M_T = M_R = M$. Let $L = L_T$ and $\Omega = \Omega_T$. Suppose the kernels of all H_{nm}'s are independent, white Gaussian random process with zero mean and unit variance. Then, the channel response is equivalent to

$$Q_{L_R} P_{\Omega_R} H P_{\Omega_T} Q_{L_T}$$

and the kernel of H is white Gaussian random process with zero mean and unit variance. If the receiver knows H, then the capacity C_{DU} satisfies

$$-\log_2 e \le \lim_{\mathsf{SNR}\to\infty}\lim_{L|\Omega|\to\infty}\left(\frac{C_{DU}}{L|\Omega|} - \log_2\mathsf{SNR}\right) \le 0 \tag{13}$$

and

$$\lim_{\mathsf{SNR}\to\infty}\lim_{L|\Omega|\to\infty}\frac{C_{DU}}{L|\Omega|\log_2\mathsf{SNR}} = 1 \tag{14}$$

To prove part (a), we make use of the far-field assumption which requires $L_T|\Delta|, L_R|\Delta| \ll 1$. Then, we directly apply eigen-decomposition on the simplied channel response and the rest of the proof is straightforward. For part (b) and (c), it requires the result from Landau and Widom [10]. In addition, waterfilling strategy is used in the proof of part (b). To prove part (c), we first decompose the operators $Q_{L_R}P_{\Omega_R}$ and $P_{\Omega_T}Q_{L_T}$ into their eigen-components. These give the bases for the operator H. In matrix form, due to the circularly symmetric property of IID Gaussian random variables, the operator $Q_{L_R}P_{\Omega_R}HP_{\Omega_T}Q_{L_T}$ is statistically the same as

$$\mathbf{S}_R\mathbf{H}\mathbf{S}_T$$

where $\mathbf{S}_R$ and $\mathbf{S}_T$ are diagonal matrices containing the square root of the eigenvalues of $P_{\Omega_R}Q_{L_R}P_{\Omega_R}$ and $P_{\Omega_T}Q_{L_T}P_{\Omega_T}$ respectively in a decreasing order. As a result, if the receiver knows $\mathbf{H}$, then the capacity is given by

$$C_{DU} = \max_{\mathrm{tr}\mathbf{K}\leq \mathsf{SNR}} \mathsf{E}_{\mathbf{H}}\left[\log_2 \det\left(\mathbf{I} + \mathbf{S}_R\mathbf{H}\mathbf{S}_T\mathbf{K}\mathbf{S}_T\mathbf{H}^\dagger\mathbf{S}_R\right)\right] \tag{15}$$

Solving for C_{DU} is difficult. Instead, we find a pair of upper and lower bounds for C_{DU}. Then, we show that the bounds are asymptotically the same.

B. Interpretations

$|\Omega|$ is the total width of the angular intervals subtended by the channel objects. It signifies the extent of channel scattering. We called this quantity the *channel angular width*. For simplicity, we will use Ω to denote the set itself and its measure interchangeably. In the line-of-sight channel, the capacity shown in Equation 11 is essentially the Friis transmission formula of standard antenna theory. It relates the received and transmitted power in terms of the sizes of the transmitting and receiving antennas and their separation. Due to the limited resources from the channel, increasing the size of the antenna systems only gives a power gain without any multiplexing benefit. In the specular channel, on the other hand, the scattering nature of the channel gives additional connectivities between the transmitter and the receiver. The larger the size of the antenna system, the better is its directivity and hence the more of these connections can be resolved. Therefore, the capacity in Equation 12 grows linearly with $L\Omega$. Ω reflects the extent of channel scattering and L reflects the resolvability of the antenna system. However, in the specular channel, since there is no angular spreading, the transmitted power needs to be scaled with $L\Omega$. In contrast, the diffuse channel has angular spreading so the transmitted power needs not to be scaled with $L\Omega$ in order to get the linear growth in capacity as shown in Equation 14.

IV. Optimum Antenna Array Configuration

The multiplexing limit derived in the last section is in an asymptotic sense. That is, it gives the optimum number of antenna elements for a large system in a given channel. In this section, we will apply the proposed channel model to investigate the optimum number of antenna elements for a practical system in two different types of channel.

First, we will consider a fully-scattered channel in which Ω equals to 2. That is, there are channel objects all around the transmitter and the receiver. This is equivalent to the conventional IID Rayleigh fading model with antenna separation of half-wavelength. Figure 1 shows the channel capacity versus the number of antenna elements for both diffuse and specular channels at different SNR. The aperture length considered is 4 wavelengths, that is, L is equal to 4. Thus, $L\Omega$ is equal to 8 which is also the number of antenna elements presumed in the conventional fading model. From the graph, we find out that at high SNR, it is possible to obtain more capacity by having more than 8 antenna elements. This is because the small eigenvalues of the composite operator $P_\Omega Q_L P_\Omega$ that are once negligible, will contribute to the usable transmission modes at high SNR.

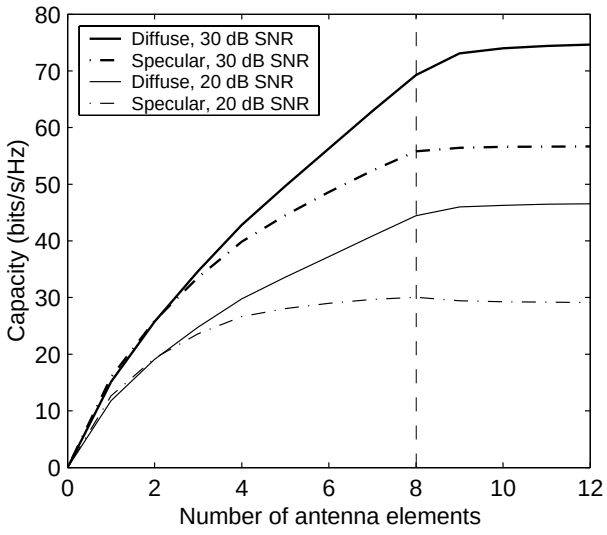

Fig. 1. Number of antenna elements vs. channel capacity for a fully scattered channel.

Second, we will consider a more realistic channel with parameters inferred from indoor channel measurements [6]. In this channel, there are 3 disjoint angular intervals, each of width $20°$. That is, M is equal to 3 and $L\Omega$ is close to 3 as well. Figure 2 shows the capacity versus the number of antenna elements. As compared to the fully-scattered channel, the capacities are almost halved. Half-wavelength antenna separation is too conservative in most scenarios. On the other hand, an $L\Omega$ number of antenna elements is too pessimistic at high SNR. This is because the disjointness in the angular intervals results in more spreading in the point spectrum of the composite operator $P_\Omega Q_L P_\Omega$. Consequently, there are substantial transmission modes that are once insignificant, become usable at high SNR.

V. Optimum Operating Frequency

The channel model proposed in Section II emphasizes on the separation of channel and antenna array characteristics. This separation allows the multiplexing limits derived in Section III to reflect the impact of channel and antenna array individually on performance limits. This separation on performance limits, in turn, allows the performance evaluation of a multiple-antenna channel in different frequency bands for a given scenario. In this section, we will demonstrate this evaluation scheme.

The channel characterization reported in [6] shows a decrease in both the number of angular intervals, M and the an-

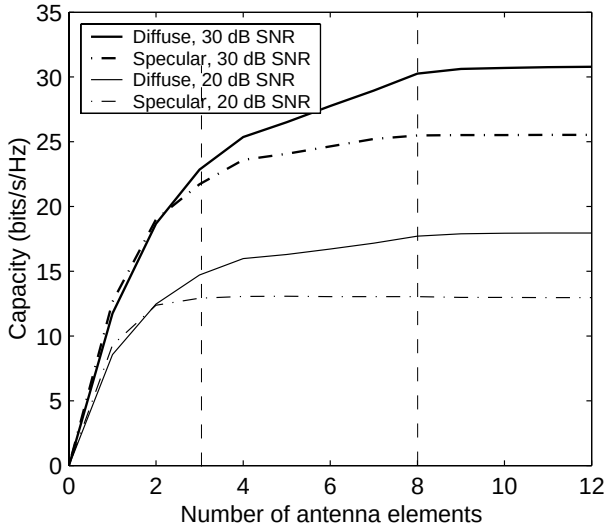

Fig. 2. Number of antenna elements vs. channel capacity for a measured indoor channel.

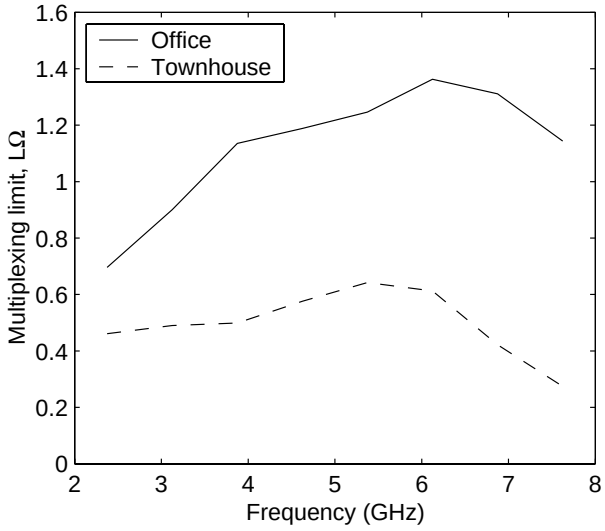

Fig. 3. Multiplexing limits vs. operating frequencies.

gular width of each interval, $|\Omega_i|$ with increasing operating frequency. The decrease in the number of angular intervals can be due to the fact that electromagnetic waves of higher frequency attenuate more after passing through or bouncing off the channel objects. The decrease in the angular interval is because at high frequency, the wavelength is small relative to the feature size of typical channel objects, so scattering appears to be more specular in nature and results in less angle spreading. After all, the channel angular width, Ω which is the product of the number of angular intervals and the width of each interval, decreases with increasing frequency. However, at the same time, the aperture length normalized to wavelength, L increases with frequency. As a result, the multiplexing limit $L\Omega$ varies with the operating frequency. Figure 3 shows the multiplexing limits versus operating frequency in an office and a townhouse environment. The channel angular width used is extracted from [6]. The graphs show that the multiplexing limit first increases with frequency and after passing an optimum frequency, then decreases. Moreover, the optimum frequencies for these particular channels are between 5 to 6 GHz. This variation in multiplexing limit counteracts the common belief that in moving to a higher operating frequency, one benefits from packing more antenna elements on a wireless device.

VI. Network Abstraction

In modeling the wave propagation mechanism detailed in Section II-B, the channel response relates the transmit directions to the receive directions. The response is non-zero at transmit beam-angle β and receive beam-angle α, whenever there is a channel object providing connectivity between these angles. In a network environment, nearby users can be viewed as another type of channel object affecting this connectivity. If the nearby user is cooperative, then it can be modeled as a relay similar to the diffused channel object. If it is non-cooperative, then it will reduce the signal-to-noise ratio in that particular pair of transmit and receive angles. As a result, depending on the incentive of the nearby users, we can abstract them following the approach demonstrated in Section II-B and carry the same analysis.

VII. Summary

In this paper, we propose a physical multiple-antenna channel model. Based on this model, we show that channel capacity grows linearly with a factor depending on the size of the antenna array entirely and another factor on the extent of channel scattering solely. This separation of antenna array and channel characteristics allow system designer to better understand and optimize system performance, for example, in choosing the number of antenna elements and the operating frequency band. Finally, we show how the proposed approach extends to a network of multiple-antenna systems.

VIII. Acknowledgement

The authors would like to acknowledge the support of MACRO and the industrial members of Berkeley Wireless Research Center.

References

[1] E. Telatar. Capacity of multi-antenna gaussian channels. *AT&T-Bell Labs Internal Techical Memo.*, June 1995.

[2] G. J. Foschini. Layered space-time architecture for wireless communication in a fading environment when using multi-element antennas. *Bell Labs Technical Journal*, pages 41–59, Autumn 1996.

[3] V. Tarokh, N. Seshadri, and A. R. Calderbank. Space-time codes for high data rate wireless communications: Performance criterion and code construction. *IEEE Transactions on Information Theory*, 44:744–65, 1998.

[4] H. G. Booker and P. C. Clemmow. The concept of an angular spectrum of plane waves, and its relation to that of polar diagram and aperture distribution. *Proc. IEE (London)*, 97:11–17, January 1950.

[5] A. A. M. Saleh and R. A. Valenzuela. A statistical model for indoor multipath propagation. *IEEE Journal on Selected Areas in Communications*, SAC-5(2):128–137, February 1987.

[6] A. Poon and M. Ho. Indoor multiple-antenna channel characterization from 2 to 8 ghz. Submitted to ICC, 2002.

[7] Q. H. Spencer, B. D. Jeffs, M. A. Jensen, and A. Lee Swindlehurst. Modeling the statistical time and angle of arrival characteristics of an indoor multipath channel. *IEEE Journal on Selected Areas in Communications*, 18:347–360, March 2000.

[8] R. Heddergott and P. Truffer. Statistical characteristics of indoor radio propagation in nlos scenarios. Technical Report COST 259, Tech. Rep. COST 259 TD(00) 024, Valencia, Spain, January 2000.

[9] T. S. Rappaport. *Wireless Communications: Principle and Practice*. Prentice Hall PTR, Upper Saddle River, NJ, 1996.

[10] H. J. Landau and H. Widom. Eigenvalue distribution of time and frequency limiting. *Journal of Mathematical Analysis and Applications*, 77:469–481, 1980.